JOURNAL OF GUIDANCE, CONTROL, AND DYNAMICS
Vol. 34, No. 5, September–October 2011

Engineering Notes

Aircraft Trajectory Optimization and Contrails Avoidance in the Presence of Winds

Banavar Sridhar*
NASA Ames Research Center,
Moffett Field, California 94035-1000
Hok K. Ng†
University of California, Santa Cruz,
Moffett Field, California 94035-1000
and
Neil Y. Chen‡
NASA Ames Research Center,
Moffett Field, California 94035-1000

DOI: 10.2514/1.53378

I. Introduction

INTEREST in the effect of aircraft condensation trails or contrails on climate change has increased in recent years. Aircraft emissions contain water vapor, carbon dioxide, and other greenhouse gases. Contrails form in the wake of aircraft for various reasons, but the most important is the emission of water vapor [1]. They appear in the atmosphere along the aircraft's trajectory at high altitude, where the ambient temperature is very low. Contrails persist in the region of atmosphere where the relative humidity with respect to ice (RHI) is greater than 100% [2]. A recent study [3] reports that persistent contrails may have a three to four times greater effect on the climate than carbon dioxide emissions. It is tempting to reroute aircraft to minimize the impact of persistent contrails on climate. This may result in longer travel times, more fuel usage, and increased carbon dioxide emissions. However, the complete effect of persistent contrails on climate change is still not known, as they have both negative and positive effects, and the resulting net effect is uncertain. The uncertainty in the effect of persistent contrails on climate forcing requires a flight trajectory optimization algorithm with fuel and contrail models that can develop alternative flight paths to enable tradeoff between persistent contrails mitigation and fuel consumption for policy makers to make acceptable aviation operation decisions.

Several new operational strategies in air traffic management have been proposed that can potentially mitigate the impact of persistent contrails on climate change. These strategies include adjusting cruise altitude in real time [4] and rerouting aircraft around regions of airspace that facilitate persistent contrails formation [5]. The study in [6] presents a methodology to optimally reroute aircraft trajectories to avoid the formation of persistent contrails with the use of mixed integer programming. However, the computational complexity is very high for problems with many obstacles and dynamic constraints. None of the current methods for avoiding contrails [6,7] consider the effect of wind on the aircraft trajectory and neglect the potential fuel savings that aircraft can gain when flying wind-optimal routes.

This study develops an algorithm to calculate a wind-optimal trajectory for cruising aircraft while avoiding the regions of airspace that facilitate persistent contrails formation, since expert panels [3] have suggested focusing on the impacts of subsonic aviation emissions at cruise altitudes in the upper troposphere and lower stratosphere. The computationally efficient optimal trajectory is derived by solving a nonlinear optimal control problem with path constraints [8]. The regions of airspace favorable to persistent contrails formation are modeled as undesirable regions that aircraft should avoid and are formulated as soft state constraints. It is shown that the dynamical equation for aircraft optimal heading is reduced to the solution of the Zermelo problem [9] in the absence of constrained airspace regions.

Section II provides the model for diagnosing regions of airspace that are susceptible for persistent contrail formation. Section III explains the optimal trajectory generation for cruising aircraft. Section IV describes the application of the trajectory optimization algorithm for calculating wind-optimal and contrails-avoidance routes. Conclusions and future work are described in Sec. V.

II. Persistent Contrails Formation Models

The formation of contrails has been under investigation since 1919 [1]. According to Appleman [10], contrails are clouds that form when a mixture of warm engine exhaust gases and cold ambient air reaches saturation with respect to water, forming liquid drops, which quickly freeze. Contrails form in the regions of airspace that have ambient relative humidity with respect to water (RHW) greater than a critical value r_{contr} [11]. Contrails can persist when the ambient air is supersaturated with respect to ice; that is, the environmental RHI is greater than 100% [2]. In this study, the regions of airspace that have RHW greater than r_{contr} and RHI greater than 100% are considered favorable to persistent contrails formation. The studies in [12,13] measure the validity of contrails formation by comparing them with satellite observation. There is general agreement between the satellite images and the persistent contrails regions predicted by the model.

The estimated critical relative humidity r_{contr} for contrails formation at a given temperature T (in Celsius) can be calculated as [11]

$$r_{\text{contr}} = \frac{G(T - T_{\text{contr}}) + e_{\text{sat}}^{\text{liq}}(T_{\text{contr}})}{e_{\text{sat}}^{\text{liq}}(T)} \tag{1}$$

where $e_{\text{sat}}^{\text{liq}}(T)$ is the saturation vapor pressure over water at a given temperature. The estimated threshold temperature (in Celsius) for contrails formation at liquid saturation is [1]

$$T_{\text{contr}} = -46.46 + 9.43\ln(G - 0.053) + 0.72\ln^2(G - 0.053) \tag{2}$$

where $G = (\text{EI}_{\text{H}_2\text{O}} C_p P)/[\varepsilon Q(1-\eta)]$. $\text{EI}_{\text{H}_2\text{O}}$ is the emission index of water vapor, and it is assumed to be 1.25; $C_p = 1004\ \text{J Kg}^{-1}\ \text{K}^{-1}$ is the isobaric heat capacity of air, P (in pascals) is the ambient air pressure, $\varepsilon = 0.6222$ is the ratio of molecular masses of water and dry air, $Q = 43 \times 10^6\ \text{J Kg}^{-1}$ is the specific combustion heat, and $\eta = 0.3$ is the average propulsion efficiency of the jet engine.

Presented as Paper 2010-9139 at the 10th Aviation Technology, Integration, and Operations Conference, Fort Worth, TX, 13–15 September 2010; received 9 December 2010; revision received 8 March 2011; accepted for publication 17 March 2011.

*Senior Scientist for Air Transportation Systems, Aviation Systems Division. Fellow AIAA.
†Senior Software Engineer, Mail Stop 210-8. Member AIAA.
‡Aerospace Research Engineer, Systems Modeling and Optimization Branch, Mail Stop 210-10. Member AIAA.

The values of r_{contr} and RHI are computed using measurements from the rapid update cycle (RUC). RUC is an operational weather prediction system developed by the National Oceanic and Atmospheric Administration for users needing frequently updated short-range weather forecasts (e.g., the U.S. aviation community). The horizontal resolution in RUC is 40 km. RUC data have 37 vertical isobaric pressure levels ranging between 100–1000 mb in 25 mb increments. The RUC produces short-range forecasts every hour. The value of r_{contr} is computed by Eqs. (1) and (2) using RUC measurements for RHW and temperatures. RUC does not provide measurements for RHI directly. Instead, RHI is calculated by the following formula:

$$\text{RHI} = \text{RHW} \cdot \frac{6.0612 e^{18.102 \cdot T/(249.52+T)}}{6.1162 e^{22.577 \cdot T/(273.78+T)}} \tag{3}$$

Note that the numerator on the right-hand side of Eq. (3) is the saturation vapor pressure over water $e_{\text{sat}}^{\text{liq}}(T)$ from the model, denoted as AERW(50, −80) in [14], and the denominator is the saturation vapor pressure over ice, from the model denoted as AERWi(0, −80) in [14].

This model will be used to compute the regions in the U.S. airspace that facilitate persistent contrails formation.

III. Optimal Trajectory on Horizontal Plane

Aircraft trajectory optimization algorithms are well known and are solutions to two-point boundary-value problems (TPBVPs) [9]. The various approximations to the solution of the TPBVPs depend on the application, and they are motivated by the desire to balance computation speed with accuracy. The cruise altitude of most commercial aircraft varies between 29,000 to 41,000 ft. The flight levels are separated by 2000 ft between two levels of flight in the same direction [1000 ft since the introduction of reduced vertical separation minima (RVSM)]. As the choice of the cruise altitude varies over a small range, the optimal aircraft trajectories in this Note are computed by repeatedly solving the horizontal plane problem.

This section develops the optimal trajectory algorithm for cruising aircraft. Section III.A presents the aircraft model and outlines the procedures for calculating optimal aircraft heading in a two-dimensional plane. Section III.B models persistent contrails formation as regions to be avoided by an aircraft and imposes a soft penalty for going through these regions.

A. Aircraft Model and Horizontal Trajectory Generation

The equations of motion in the horizontal plane are

$$\dot{x} = V\cos\theta + u(x,y) \tag{4}$$

$$\dot{y} = V\sin\theta + v(x,y) \tag{5}$$

$$\dot{m} = -f \tag{6}$$

subject to the conditions that $Th = D$ and $\gamma = 0$; and the boundary constraints that $x(t_0) = x_0$, $y(t_0) = y_0$ and $x(t_f) = x_f$, $y(t_f) = y_f$. Variables x and y are the aircraft position in rectangular coordinates, V is airspeed, θ is heading angle, m is aircraft mass, f is fuel flow rate, Th is thrust, and D is drag. The x component of the wind velocity is $u(x,y)$, and the y component of the wind velocity is $v(x,y)$.

The horizontal trajectory is optimized by determining the heading angle that minimizes a cost function and satisfies the physical system constraints. The cost function contains components that penalize traveling time, fuel burn, and flying through penalty areas [15]. The cost function is defined as

$$J = \int_{t_0}^{t_f} \{C_t + C_f f + C_r r(x,y)\}\,\mathrm{d}t \tag{7}$$

where C_t is the cost coefficient of time, C_f is the cost coefficient of fuel, f is fuel flow rate, C_r is the cost coefficient of penalty areas, and $r(x,y)$ is the penalty function. Section III.B discusses the penalty function in more detail. Pontryagin's minimum principle [9] is applied to determine the control input that minimizes the cost function. The heading angle θ is the control available for aircraft during cruise. The Hamiltonian for this problem is defined as

$$\begin{aligned} H = {} & C_t + C_f f + C_r r(x,y) + \lambda_x[V\cos\theta + u(x,y)] \\ & + \lambda_y[V\sin\theta + v(x,y)] + \lambda_m(-f) \end{aligned} \tag{8}$$

where λ_x, λ_y, and λ_m are the costate parameters. The study in [16] determined the value of λ_m to be negligible during the cruise portion of flight for transport-class aircraft. The Hamiltonian for the reduced-order model is formulated as

$$\begin{aligned} H = {} & C_t + C_f f + C_r r(x,y) + \lambda_x[V\cos\theta + u(x,y)] \\ & + \lambda_y[V\sin\theta + v(x,y)] \end{aligned} \tag{9}$$

For an extremum to exist, the optimal heading angle satisfies

$$\frac{\partial H}{\partial\theta} = 0, \qquad t_0 \le t \le t_f \Rightarrow \lambda_x \sin\theta = \lambda_y \cos\theta \Rightarrow \tan\theta = \frac{\lambda_y}{\lambda_x} \tag{10}$$

and the necessary conditions for optimality are

$$\begin{aligned} & H^* = \min\{H\}, \qquad \text{in general} \qquad H^* = 0, \\ & \text{free terminal time, } t_f \end{aligned} \tag{11}$$

Solve Eqs. (10) and (11) for the costate parameters λ_x and λ_y when the Hamiltonian is zero to obtain

$$\lambda_x = \frac{-[C_t + C_f f + C_r r(x,y)]\cos\theta}{V + u(x,y)\cos\theta + v(x,y)\sin\theta} \tag{12}$$

$$\lambda_y = \frac{-[C_t + C_f f + C_r r(x,y)]\sin\theta}{V + u(x,y)\cos\theta + v(x,y)\sin\theta} \tag{13}$$

The costate equations are

$$\begin{aligned} \dot{\lambda}_x = -\frac{\partial H}{\partial x} \Rightarrow -\dot{\lambda}_x = {} & C_r \frac{\partial r(x,y)}{\partial x} + \lambda_x\left(\frac{\partial u(x,y)}{\partial x}\right) \\ & + \lambda_y\left(\frac{\partial v(x,y)}{\partial x}\right) \end{aligned} \tag{14}$$

$$\begin{aligned} \dot{\lambda}_y = -\frac{\partial H}{\partial y} \Rightarrow -\dot{\lambda}_y = {} & C_r \frac{\partial r(x,y)}{\partial y} + \lambda_x\left(\frac{\partial u(x,y)}{\partial y}\right) \\ & + \lambda_y\left(\frac{\partial v(x,y)}{\partial y}\right) \end{aligned} \tag{15}$$

Equations (10), (14), and (15) are known as the Euler–Lagrange equations. As shown in the Appendix, the dynamical equation for the optimal aircraft heading is governed by Eqs. (10–16), and the heading angle θ is the solution to the differential equation

$$\begin{aligned} \dot{\theta} = {} & \frac{(V + u(x,y)\cos\theta + v(x,y)\sin\theta)}{[C_t + C_f f + C_r r(x,y)]}\left(-C_r \sin\theta \frac{\partial r(x,y)}{\partial x}\right. \\ & \left. + C_r \cos\theta \frac{\partial r(x,y)}{\partial y}\right) + \sin^2\theta\left(\frac{\partial v(x,y)}{\partial x}\right) \\ & + \sin\theta\cos\theta\left(\frac{\partial u(x,y)}{\partial x} - \frac{\partial v(x,y)}{\partial y}\right) - \cos^2\theta\left(\frac{\partial u(x,y)}{\partial y}\right) \end{aligned} \tag{16}$$

Note that this equation is reduced to that in the Zermelo problem [9] when $C_r = 0$. Solve Eqs. (4), (5), and (16) simultaneously to obtain the optimal path. The initial heading angle at t_0 must be picked correctly for a particular origin and destination pair.

Equations (4), (5), and (16) convert the TPBVP to an initial value problem. Given the origin and destination of an aircraft, the optimal aircraft trajectory is determined by generating a field of extremals for different values of θ_0. The optimal path is given by the extremal that goes through the destination point (x_f, y_f), and the time at which it goes through the destination point determines the value of t_f.

Our study applied the shooting method modified from that in [17] to search for both θ_0 and t_f given x_f and y_f, such that the aircraft trajectory minimizes the overall performance index in Eq. (7). The first step in searching for the optimal heading is to define the search space that occupies a region involving the starting position (x_0, y_0) and the destination position (x_f, y_f). Integrate Eqs. (4), (5), and (16) forward using some initial guesses for θ_0. The integration terminates for each initial angle when the trajectory reaches the destination or intersects the search space boundary. The distance between the destination and the intersection are used to update the initial guess for the next iteration if the destination is not reached. At the end of the search, the value of t_f is determined by the time at which the trajectory goes through the destination.

B. Contrails as Penalty Areas

Persistent contrails are modeled using penalty functions as areas to be avoided by an aircraft to reduce the potential impact on climate. The penalty functions enable a systematic way of generating aircraft trajectories that avoids the contrails formation areas by varying amounts. The cost due to persistent contrails formation in the cost function is defined as

$$J_r = \int_{t_0}^{t_f} C_r r(x, y)\, \mathrm{d}t \tag{17}$$

The penalty function $r(x, y)$ is the penalties that an aircraft can encounter along the flight trajectory from the origin to destination. In general, there are multiple regions in the en route airspace that favor persistent contrails formation. The penalty can be determined by one of the following functions:

1) The radial penalty function is

$$r(x, y) = \sum_i \frac{1}{d_i} \tag{18}$$

or

$$r(x, y) = \sum_i \frac{1}{d_i^2} \tag{19}$$

where d_i is distance between the aircraft and the center of ith region that potentially forms persistent contrails.

2) The uniform penalty function is

$$r(x, y) = \begin{cases} \text{constant} & \text{aircraft in penalty area} \\ 0 & \text{otherwise} \end{cases} \tag{20}$$

In this study, optimal trajectories will be generated using the penalty function defined in Eq. (19). In addition, there are many regions in the National Airspace System that can potentially form persistent contrails. Some are far away from the aircraft and will not be encountered by the aircraft. Some are expected to be encountered, but the area is too large for aircraft to completely avoid. Identifying the right subset of contrails and avoiding the region by an appropriate level are important for policy makers to make operational decisions and tradeoffs.

C. Aircraft Fuel Consumption Model

This study applies the fuel consumption model in Eurocontrol's Base of Aircraft Data (BADA) Revision 3.6 [18] to compute cruising aircraft fuel consumption. The following equation calculates fuel burn for aircraft during cruise

$$f_c = t \cdot \mathrm{SFC} \cdot Th \tag{21}$$

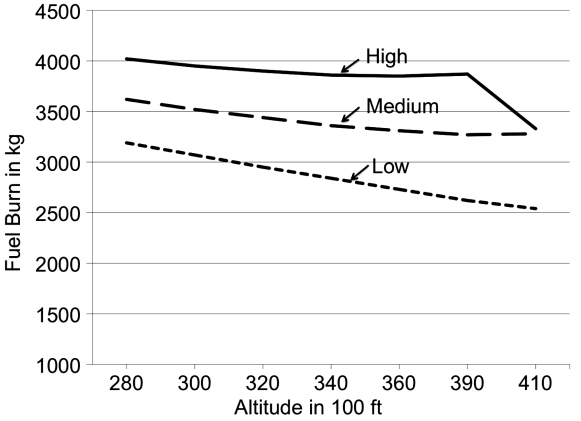

Fig. 1 Fuel flow as a function of altitude.

where f_c is the fuel burn during cruise, t is elapsed time, Th is thrust, and SFC is the specific fuel consumption. As an example, in Fig. 1, the fuel burn (in kilograms) for a typical short to medium jet airliner from Chicago to New York is shown as a function of altitude for three different weights: low, medium, and high.

IV. Results

This section presents results based on applying the optimal trajectory algorithm to calculate an aircraft trajectory in the presence of winds that avoids regions of airspace that facilitate persistent contrails formation. The trajectory computations are done using traffic and atmospheric data in the continental United States for 24 May 2007. The data for windspeed and direction are obtained from RUC. The solid and dotted polygons in Fig. 2 depict the areas at 37,000 ft above sea level in the U.S. national airspace where atmospheric conditions are favorable for persistent contrails formation at 0600 and 0800 hrs Eastern Daylight Time (EDT) on 24 May 2007, respectively. The critical relative humidity and RHI values are computed using Eq. (1–3) in Sec. II with RHW values, pressure, and temperature data obtained from RUC. Figure 2 shows that the location, shape, and size of potential contrail regions vary with time.

A. Chicago (O'Hare International Airport) to Washington (Dulles International Airport)

The trajectory design in this example focuses on avoiding the potential contrails regions between Chicago and Washington, D.C. At each altitude, C_r is varied from zero to a value where the optimal trajectory completely avoids the contrail region. The time for the wind-optimal route, the time through contrail regions, the value of C_r to avoid contrails, and the extra fuel consumption are computed at each altitude. This process is repeated at all the six altitudes. Three optimal trajectories from Chicago O'Hare Airport (ORD) to Washington Dulles Airport (IAD) are shown in Fig. 3 for flights with cruising altitudes equal to 37,000 ft. The cruising speed is assumed to be 420 n mile/h (778 km/h). The arrows represent the wind directions, obtained from RUC, at 0600 hrs EDT on 24 May 2007. The arrow sizes are plotted in proportion to the wind magnitudes. The wind-optimal trajectory is generated using Eqs. (4), (5), and (16) by setting $C_r = 0$. Two optimal trajectories in addition to the wind-optimal route are also plotted in Fig. 3. The area favorable to persistent contrails formation is surrounded by the black polygon that is identified as a potential penalty area to the aircraft. The cross is the center of the penalty area. The position of penalty centers and the aircraft position are used in Eq. (19) to calculate the distance and the penalty cost. In this example, the cost coefficient of time is chosen as $C_t = 20$. The cost coefficient of penalty C_r is equal to 0.5 and 2.0. Note that the penalty coefficient C_r is treated as a design parameter. The choice of this parameter is not unique and depends on the definition of the penalty function itself. The optimal route with $C_r = 2.0$ completely avoids the contrail polygons near the departure

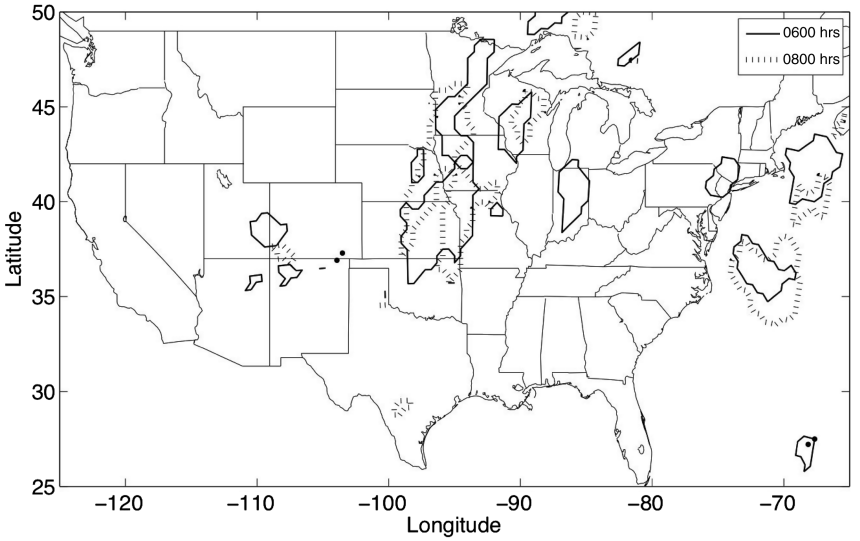

Fig. 2 Regions of airspace at 37,000 ft, where favorable to persistent contrails formation occurs at 0600 and 0800 hrs EDT on 24 May 2007.

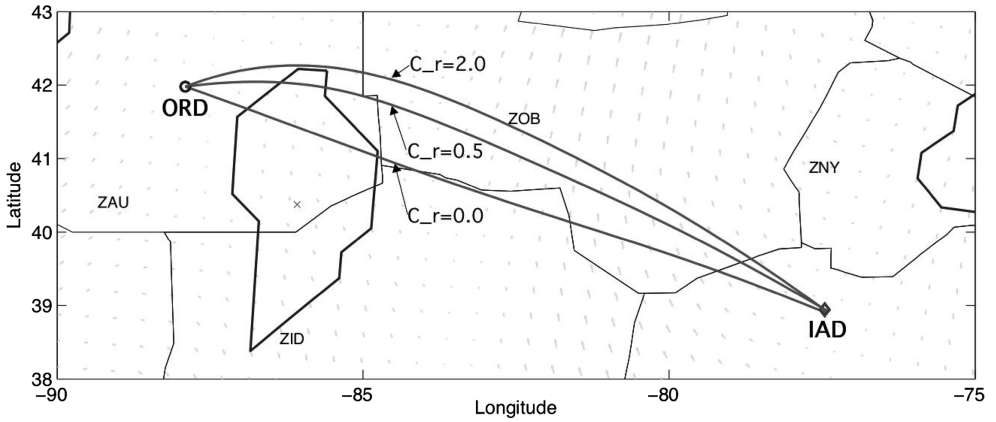

Fig. 3 Optimal trajectories at 37,000 ft from ORD to IAD with different design parameters [ZAU: Chicago air route traffic control center (ARTCC); ZID: Indianapolis ARTCC; ZOB: Cleveland ARTCC; ZNY ARTCC].

airport. The optimal route with $C_r = 0.5$ only partially avoids the polygons but is shorter. In this case, there is a tradeoff between flying a shorter route with more persistent contrails formation versus flying a longer route with less persistent contrails formation. The performance of optimal trajectories is evaluated by investigating the total travel time and the time associated traveling through regions of persistent contrails formation.

Optimal aircraft trajectories are generated for six different altitudes between 29,000 and 39,000 ft. Figure 4 shows the results for the six wind-optimal trajectories. The sum of dark gray and light gray bars represents the total travel time for each trajectory, and the light gray bar represents the amount of time that a flight travels inside the regions of airspace favorable to persistent contrails formation. The wind-optimal trajectories at 29,000, 31,000, 33,000, and 35,000 ft do not intercept any region of airspace that facilitates persistent contrails formation. The flights at these cruising altitudes should fly the wind-optimal trajectories that minimize fuel burn and emissions. Flying wind-optimal trajectories at 37,000 and 39,000 ft will potentially cause persistent contrails formation. Optimal contrails-avoidance trajectories at these altitudes are generated by increasing the value of C_r from 0 to 2 with increments equal to 0.1.

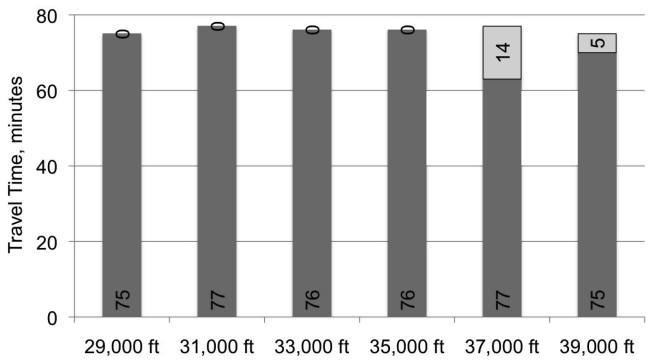

Fig. 4 Travel time for wind-optimal routes from ORD to IAD and length of periods favorable to persistent contrails formation at six different altitudes.

The second columns for altitudes of 37,000 and 39,000 ft in Table 1 show the value of C_r, the total fuel consumption for the contrails-avoidance trajectory, and the additional fuel burn compared with that of wind-optimal trajectory. The remaining columns show the data for wind-optimal trajectories. Flying a contrails-avoidance trajectory requires 1.81% additional fuel burn at 37,000 and 39,000 ft, respectively, to avoid potentially 14 and 5 min of persistent contrails formation. More optimal trajectories can be calculated with various choice of C_r.

B. Optimal Trajectories for 12 City Pairs

This section analyzes the wind-optimal and contrails-avoidance trajectories for 12 origin-destination pairs for a period of 24 h starting from 0600 hrs EDT on 24 May 2007. The same city pairs were used by the Federal Aviation Administration to assess the impact of implementation of RVSM on aircraft-related fuel burn and emissions

Table 1 Trajectories from ORD to IAD

	Altitude, ft							
	29,000[a]	31,000[a]	33,000[a]	35,000[a]	37,000		39,000	
C_r	0	0	0	0	0[a]	2.0[b]	0[a]	0.6[b]
Contrails, min	0	0	0	0	14.0[a]	0[b]	5[a]	0[b]
Fuel burn, kg	3020	2978	2885	2814	2756[a]	2806[b]	2658[a]	2706[b]
Additional fuel burn, %	0	0	0	0	0[a]	1.81[b]	0[a]	1.81[b]

[a]Wind-optimal trajectories.
[b]Contrails-avoidance trajectories.

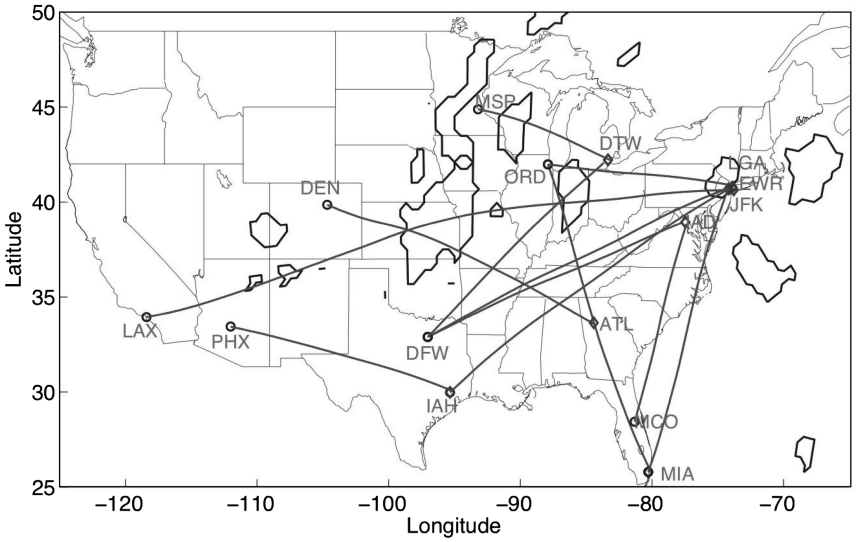

Fig. 5 Wind-optimal trajectories for eastbound flights for 12 city pairs at 37,000 ft, 0600 hrs EDT, on 24 May 2007.

Table 2 Average persistent contrails formation time (minutes) for optimal aircraft trajectories for 12 cities on 24 May 2007[a]

	Maximum additional fuel consumption, %										
City pair	0	2		4		6		8		8+	
LAX to JFK	7.8	3.8	1.6	2.8	0.4	2.5	0.1	2.0	0.0	0.2	0.0
JFK to LAX	10.8	5.3	1.8	3.6	0.4	1.3	0.0	1.2	0.0	0.5	0.0
ATL to DEN	8.1	5.5	3.4	4.4	0.8	3.6	0.0	3.0	0.0	1.8	0.0
DEN to ATL	6.3	4.6	2.9	3.8	0.7	3.6	0.0	3.4	0.0	4.1	0.0
DTW to DFW	2.4	1.6	0.4	1.1	0.0	1.0	0.0	0.8	0.0	0.5	0.0
DFW to DTW	3.2	2.5	1.2	1.8	0.2	1.1	0.0	0.9	0.0	0.5	0.0
PHX to IAH	2.2	1.7	1.6	1.6	0.1	1.4	0.0	1.4	0.0	1.3	0.0
IAH to PHX	3.3	2.5	0.0	2.2	0.0	2.0	0.0	2.0	0.0	1.9	0.0
DFW to LGA	1.5	1.1	0.6	0.7	0.1	0.6	0.0	0.5	0.0	0.4	0.0
LGA to DFW	1.6	1.1	0.4	0.7	0.0	0.4	0.0	0.2	0.0	0.1	0.0
DFW to IAD	1.3	0.8	0.4	0.6	0.2	0.5	0.0	0.5	0.0	0.3	0.0
IAD to DFW	1.2	0.8	0.4	0.7	0.0	0.5	0.0	0.4	0.0	0.2	0.0
ORD to LGA	0.9	0.5	0.3	0.4	0.1	0.3	0.0	0.3	0.0	0.3	0.0
LGA to ORD	1.3	0.6	0.3	0.5	0.1	0.3	0.0	0.3	0.0	0.3	0.0
MSP to DTW	0.7	0.5	0.3	0.5	0.2	0.3	0.0	0.3	0.0	0.2	0.0
DTW to MSP	0.5	0.5	0.1	0.4	0.0	0.2	0.0	0.2	0.0	0.1	0.0
IAH to EWR	0.8	0.6	0.1	0.5	0.0	0.5	0.0	0.4	0.0	0.3	0.0
EWR to IAH	0.2	0.1	0.0	0.1	0.0	0.0	0.0	0.0	0.0	0.0	0.0
ORD to MIA	0.4	0.1	0.1	11.3	0.0	9.8	0.0	8.8	0.0	3.1	0.0
MIA to ORD	0.3	0.1	0.0	0.0	0.0	0.0	0.0	0.0	0.0	0.0	0.0
MIA to EWR	0.0	0.0	0.0	0.0	0.0	0.0	0.0	0.0	0.0	0.0	0.0
EWR to MIA	0.0	0.0	0.0	0.0	0.0	0.0	0.0	0.0	0.0	0.0	0.0
IAD to MCO	0.0	0.0	0.0	0.0	0.0	0.0	0.0	0.0	0.0	0.0	0.0
MCO to IAD	0.0	0.0	0.0	0.0	0.0	0.0	0.0	0.0	0.0	0.0	0.0

[a]LAX denotes Los Angeles International Airport, JFK denotes John F. Kennedy International Airport, DEN denotes Denver International Airport, ATL denotes Hartsfield-Jackson Atlanta International Airport, DFW denotes Dallas-Fort Worth International Airport, PHX denotes Sky Harbor International Airport, and LGA denotes LaGuardia Airport.

[19]. This part of the study adapts the standard in RVSM and assumes that the cruising altitudes are between 29,000 and 41,000 ft. Eastbound aircraft fly odd 1000s of feet, while westbound traffic fly even 1000s of feet. Figure 5 shows the wind-optimal trajectories for the eastbound flights at 37,000 ft at 0600 hrs EDT. Black polygons depict the areas favorable to persistent contrails formation.

The optimal aircraft trajectories are generated at the beginning of each hour on 24 May 2007 using hourly updated weather data from RUC. Six flight levels are considered for each direction of air traffic for each city pair. A group of 21 optimal aircraft trajectories are calculated for each flight level by increasing the value of C_r from 0 to 2 with increments equal to 0.1. The cost coefficient of time is chosen as $C_t = 20$ for each case. The cruising speed is assumed to be 420 n mile/h. The fuel consumption for each aircraft trajectory is calculated using BADA formulas by assuming that the aircraft are short- to medium-range jet airliners with medium weight. In each group, the additional fuel consumption of each optimal trajectory is obtained by comparing its fuel burnt with that of its wind-optimal trajectory ($C_r = 0$). The persistent contrails formation time associated to each trajectory is also recorded.

A total of six bins is defined such that the aircraft trajectories can be categorized based on their additional fuel consumption. The first bin contains the wind-optimal trajectory, which is the baseline for fuel use comparison and corresponds to trajectories that require 0% of additional fuel consumption. The second bin contains aircraft trajectories that consume less than 2% additional fuel, the third bin contains those consuming less than 4%, etc. The sixth bin has trajectories that burn more than 8% of fuel. In each bin, the optimal trajectory that has the least amount of persistent contrails formation time is selected to represent the bin. Note that there are six bins for each group of trajectories and six groups for each direction of air traffic every hour. The average persistent contrails formation times for the optimal trajectories are summarized in Table 2. The first column of data presents the average contrails formation time measured in minutes for the wind-optimal trajectories. The average is taken over six flight levels and a period of 24 h for each direction. Flying wind-optimal routes on any of the six flight levels between Miami International Airport (MIA) and Newark International Airport (EWR) or between IAD and Orlando International Airport (MCO) does not induce persistent contrails formation during the day under consideration. The contrails formation time is less than a minute on average for the city pairs such as Minneapolis-Saint Paul International Airport (MSP)–DTW, George Bush Intercontinental Airport (IAH)–EWR, and ORD–MIA. The first columns of data under 2, 4, 6, 8, and 8+ present the average contrails formation time for the optimal contrails-avoidance trajectories. These optimal trajectories consume different amounts of additional fuel at each bin or column. In general, the flights, which can afford additional fuel burn, induce fewer contrails, since they have more routes to choose from. The second columns of data under 2, 4, 6, 8, and 8+ present the average contrails formation time for the optimal contrails-avoidance trajectories on the optimized altitudes that produce the least amount of contrails. The flights, which can select the flying altitudes, induce much fewer contrails given the same amount of extra fuel.

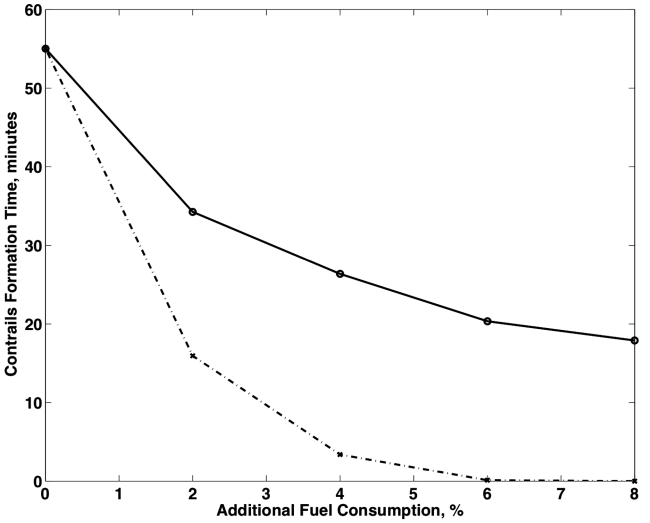

Fig. 6 Tradeoff curves between fuel consumption and contrail avoidance.

The data in Table 2 can be converted into the actual amount of extra fuel consumed by various flights, and then it can be aggregated to produce a simplified total extra fuel consumption versus total minutes through the contrail regions for all the flights between the 12 city pairs. Figure 6 shows the curves with (solid curve) and without (dashed–dotted curve) altitude optimization. The figure shows that, when altitude is optimized, a 2% increase in total fuel consumption can reduce the total travel times through contrail regions from 55 to 16 min. Allowing further increase in fuel consumption does not result in a proportionate reduction in contrail travel times. Without altitude optimization, the reduction in contrail travel times is gradual with the increase in total fuel consumption. The data in Table 2 can be used to develop optimal fleet allocation and scheduling strategies to minimize the travel time through contrails.

V. Conclusions

This study develops an algorithm to calculate wind-optimal trajectories for aircraft while avoiding the regions of airspace that facilitate persistent contrails formation. The optimal trajectory is derived by solving a nonlinear optimal control problem with path constraints. The operational strategies investigated in this study for minimizing aviation impacts on climate change include flying wind-optimal routes, avoiding complete or partial persistent contrails formation, and altering cruising altitudes. The tradeoff between persistent contrails formation and additional travel time are investigated at six different cruising altitudes for flights from Chicago to Washington. The additional travel times required for completely avoiding persistent contrails formation at various flight altitudes is about 1.8% for flights from Chicago to Washington. The tradeoff between persistent contrails formation and additional fuel consumption is investigated, with and without altitude optimization, for 12 city pairs in the continental United States. When altitude is optimized, a 2% increase in total fuel consumption can reduce the total travel times through contrail regions by more than 70%. Allowing a further increase in fuel consumption does not seem to result in a proportionate decrease in contrail travel times. Allowing further increase in fuel consumption results in more reduction in contrail travel times. Without altitude optimization, the reduction in contrail travel times is gradual with an increase in total fuel consumption.

The results in this Note were based on traffic for a single day and used the same type of aircraft on all routes. The results can be modified using the complete traffic and weather data for extended periods of time to get a better understanding of the complex relation between fuel efficiency and the impact on the environment.

Appendix

The dynamical equation for the optimal aircraft heading is obtained using Eqs. (11–16). Differentiating both sides of Eq. (11) gives

$$\sec^2\theta\dot{\theta} = \frac{\dot{\lambda_y}\lambda_x - \lambda_y\dot{\lambda_x}}{\lambda_x^2} \Rightarrow \dot{\theta} = \frac{\cos^2\theta[\dot{\lambda_y}\lambda_x - \lambda_y\dot{\lambda_x}]}{\lambda_x^2} \tag{A1}$$

Substitute

$$\lambda_x = \frac{-[C_t + C_f f + C_r r(x,y)]\cos\theta}{V + u(x,y)\cos\theta + v(x,y)\sin\theta}$$

and

$$\lambda_y = \frac{-[C_t + C_f f + C_r r(x,y)]\sin\theta}{V + u(x,y)\cos\theta + v(x,y)\sin\theta}$$

from Eqs. (12) and (13) into Eq. (A1) to get

$$\dot{\theta} = \frac{(V + u(x,y)\cos\theta + v(x,y)\sin\theta)(-\dot{\lambda}_y \cos\theta + \dot{\lambda}_x \sin\theta)}{[C_t + C_f f + C_r r(x,y)]} \tag{A2}$$

We have, from Eqs. (14) and (15),

$$\begin{aligned}\dot{\lambda}_x &= -C_r \frac{\partial r(x,y)}{\partial x} - \lambda_x \left(\frac{\partial u(x,y)}{\partial x}\right) - \lambda_y \left(\frac{\partial v(x,y)}{\partial x}\right) \\ &= -C_r \frac{\partial r(x,y)}{\partial x} + \frac{[C_t + C_f f + C_r r(x,y)]\cos\theta}{V + u(x,y)\cos\theta + v(x,y)\sin\theta}\left(\frac{\partial u(x,y)}{\partial x}\right) \\ &+ \frac{[C_t + C_f f + C_r r(x,y)]\sin\theta}{V + u(x,y)\cos\theta + v(x,y)\sin\theta}\left(\frac{\partial v(x,y)}{\partial x}\right),\end{aligned}$$

and

$$\begin{aligned}\dot{\lambda}_y &= -C_r \frac{\partial r(x,y)}{\partial y} - \lambda_x \left(\frac{\partial u(x,y)}{\partial y}\right) - \lambda_y \left(\frac{\partial v(x,y)}{\partial y}\right) \\ &= -C_r \frac{\partial r(x,y)}{\partial y} \\ &+ \frac{[C_t + C_f f + C_r r(x,y)]\cos\theta}{V + u(x,y)\cos\theta + v(x,y)\sin\theta}\left(\frac{\partial u(x,y)}{\partial y}\right) \\ &+ \frac{[C_t + C_f f + C_r r(x,y)]\sin\theta}{V + u(x,y)\cos\theta + v(x,y)\sin\theta}\left(\frac{\partial v(x,y)}{\partial y}\right)\end{aligned}$$

Splitting the right-hand side of Eq. (A2) into two parts, we get

$$\begin{aligned}&\frac{[V + u(x,y)\cos\theta + v(x,y)\sin\theta](-\dot{\lambda}_y \cos\theta)}{[C_t + C_f f + C_r r(x,y)]} \\ &= \left[C_r \frac{\partial r(x,y)}{\partial y}\right] \frac{\cos\theta[V + u(x,y)\cos\theta + v(x,y)\sin\theta]}{[C_t + C_f f + C_r r(x,y)]} \\ &- \cos^2\theta \left(\frac{\partial u(x,y)}{\partial y}\right) - \cos\theta\sin\theta \left(\frac{\partial v(x,y)}{\partial y}\right)\end{aligned} \tag{A3}$$

$$\begin{aligned}&\frac{[V + u(x,y)\cos\theta + v(x,y)\sin\theta](\dot{\lambda}_x \sin\theta)}{[C_t + C_f f + C_r r(x,y)]} \\ &= \left[-C_r \frac{\partial r(x,y)}{\partial x}\right] \frac{\sin\theta[V + u(x,y)\cos\theta + v(x,y)\sin\theta]}{[C_t + C_f f + C_r r(x,y)]} \\ &+ \sin\theta\cos\theta \left(\frac{\partial u(x,y)}{\partial x}\right) + \sin^2\theta \left(\frac{\partial v(x,y)}{\partial x}\right)\end{aligned} \tag{A4}$$

Summing Eqs. (A3) and (A4) to obtain dynamical equation for the optimal heading,

$$\begin{aligned}\dot{\theta} &= \frac{[V + u(x,y)\cos\theta + v(x,y)\sin\theta]}{[C_t + C_f f + C_r r(x,y)]}\left[-C_r \sin\theta \frac{\partial r(x,y)}{\partial x}\right. \\ &\left. + C_r \cos\theta \frac{\partial r(x,y)}{\partial y}\right] + \sin^2\theta \left(\frac{\partial v(x,y)}{\partial x}\right) \\ &+ \sin\theta\cos\theta \left(\frac{\partial u(x,y)}{\partial x} - \frac{\partial v(x,y)}{\partial y}\right) - \cos^2\theta \left(\frac{\partial u(x,y)}{\partial y}\right)\end{aligned} \tag{A5}$$

When C_r is zero, Eq. (A5) is reduced to a solution in the Zermelo problem.

References

[1] Schumann, U., "On Conditions for Contrail Formation from Aircraft Exhausts," *Meteorologische Zeitschrift; Acta Scientiarium Naturalium Universitatis Normalis Hunanensis*, Vol. 5, Feb. 1996, pp. 4–23.

[2] Duda, D. P., Minnis, P., and Palikonda, R., "Estimated Contrail Frequency and Coverage over the Contiguous United States from Numerical Weather Prediction Analyses and Flight Track Data," *Meteorologische Zeitschrift; Acta Scientiarium Naturalium Universitatis Normalis Hunanensis*, Vol. 14, No. 4, Aug. 2005, pp. 537–548. doi:10.1127/0941-2948/2005/0050

[3] Waitz, I., Townsend, J., Cutcher-Gershenfeld, J., Greitzer, E., and Kerrebrock, J., "Report to the United States Congress: Aviation and the Environment, A National Vision, Framework for Goals and Recommended Actions," *Partnership for Air Transportation Noise and Emissions Reduction*, Massachusetts Ints. of Technology, Cambridge, MA, Dec. 2004, p. 18.

[4] Klima, K., "Assessment of a Global Contrail Modeling Method and Operational Strategies for Contrail Mitigation," M. S. Thesis, Massachusetts Ints. of Technology, Cambridge, MA, 2005.

[5] Mannstein, H., Spichtinger, P., and Gierens, K., "A Note on How to Avoid Contrail Cirrus," *Transportation Research. Part D, Transport and Environment*, Vol. 10, No. 5, 2005, pp. 421–426. doi:10.1016/j.trd.2005.04.012

[6] Campbell, S. E., Neogi, N. A., and Bragg, M. B., "An Optimal Strategy for Persistent Contrail Avoidance," AIAA Guidance, Navigation, and Control Conference, Honolulu, HI, AIAA Paper 2008-6515, 2008.

[7] Gierens, K., Lim, L., and Eleftheratos K., "A Review of Various Strategies for Contrail Avoidance," *Open Atmosphere Science Journal*, Vol. 2, No. 1, 2008, pp. 1–7. doi:10.2174/1874282300802010001

[8] Naidu, D. S., and Calise, A. J., "Singular Perturbations and Time Scales in Guidance and Control of Aerospace Systems: A Survey," *Journal of Guidance, Control, and Dynamics*, Vol. 24, No. 6, Nov.–Dec. 2001, pp. 1057–1078. doi:10.2514/2.4830

[9] Bryson, A. E., and Ho, Y. C., *Applied Optimal Control*, Taylor and Francis, Levittown, PA, 1975, pp. 42–89, Chap. 2.

[10] Appleman, H., "The Formation of Exhaust Condensation Trails by Jet Aircraft," *Bulletin of the American Meteorological Society*, Vol. 34, 1953, pp. 14–20.

[11] Ponater, M., Marquart, S., and Sausen, R., "Contrails in a Comprehensive Global Climate Model: Parameterization and Radiative Forcing Results," *Journal of Geophysical Research*, Vol. 107, No. D13, 2002, Paper 4164. doi:10.1029/2001JD000429

[12] Degrand, J. Q., Carleton, A. M., Travis, D. J., and Lamb, P. J., "A Satellite-Based Climate Description of Jet Aircraft Contrails and Associations with Atmospheric Conditions, 1977–79," *Journal of Applied Meteorology*, Vol. 39, No. 9, 2000, pp. 1434–1459. doi:10.1175/1520-0450(2000)039<1434:ASBCDO>2.0.CO;2

[13] Palikonda, R., Minnis, P., Duda, D. P., and Mannstein, H., "Contrail Coverage Derived from 2001 AVHRR Data Over the Continental United States of America and Surrounding Areas," *Meteorologische Zeitschrift;Acta Scientiarium Naturalium Universitatis Normalis Hunanensis*, Vol. 14, No. 4, Aug. 2005, pp. 525–536. doi:10.1127/0941-2948/2005/0051

[14] Alduchov, O. A., and Eskridge, R. E., "Improved Magnus form Approximation of Saturation Vapor Pressure," *Journal of Applied Meteorology*, Vol. 35, No. 4, 1996, pp. 601–609. doi:10.1175/1520-0450(1996)035<0601:IMFAOS>2.0.CO;2

[15] Vian, J. L., and Moore, J. R., "Trajectory Optimization with Risk Minimization for Military Aircraft," *Journal of Guidance, Control, and Dynamics*, Vol. 12, No. 3, May–June 1989, pp. 311–317. doi:10.2514/3.20410

[16] Burrows, J. W., "Fuel-Optimal Aircraft Trajectories with Fixed Arrival Times," *Journal of Guidance, Control, and Dynamics*, Vol. 6, No. 1, Jan.–Feb. 1983, pp. 14–19. doi:10.2514/3.19796

[17] Press, W. H., Teukolsky, S. A., Vetterling, W. T., and Flannery, B. P., "Two Point Boundary Value Problems," *Numerical Recipes in C: The Art of Scientific Computing*, 2nd ed., Cambridge Univ. Press, Cambridge, England, U.K., 1992, pp. 753–787.

[18] "*User Manual for the Base of Aircraft Data (BADA), Revision 3.6*," Eurocontrol Experimental Center Note 10/04, Project ACE-C-E2, Brussels, Sept. 2004.

[19] "Benefit Analysis and Report for Domestic Reduced Vertical Separation Minimum (DRVSM)," Federal Aviation Administration Air Traffic Organization System Operations Services, CDM/DRVSM Work Group Report, Sept. 2005.